Lasers in Manufacturing Conference 2025

Influence of in-situ high-speed milling within a hybrid additive manufacturing approach on the fatigue behaviour of Inconel 718 lattice structures

David Sommer[a,*], Maximilian Peters[a], Cemal Esen[b], Ralf Hellmann[a]

[a]*Applied Laser and Photonics group, University of Applied Sciences Aschaffenburg, Wuerzburger Str. 45, 63743 Aschaffenburg, Germany*
[b]*Applied Laser Technologies, Ruhr University Bochum, Universitaetsstr. 150, 44801 Bochum, Germany*

Abstract

As lattice structures in various designs are used in additive manufacturing for lightweight components, the mechanical characterisation and fracture behaviour is of upmost importance for their industrial application. In this study, the fatigue behaviour of Inconel 718 lattice structures is evaluated, comparing sole PBF-LB/M to a hybrid additive manufacturing process combining PBF-LB/M with in-situ high-speed milling. At first, the static and dynamic mechanical load behaviour of different packing densities is analysed, determining the compressive strength and the endurance limit. Secondly, hybrid additive manufactured components are compared to PBF-LB/M built parts with respect to these mechanical properties, revealing improved compressive properties and modified regimes of fatigue. In addition, differences in fracture behaviour are qualified by fractographic and surface analysis. Overall, it can be summarized that the mechanical load characteristics, especially the fatigue behaviour, are improved for hybrid additively manufactured components with a superior surface quality of Ra < 1 µm.
Keywords: Hybrid Additive Manufacturing; Lattice Structures; Fatigue Behaviour; Inconel 718;

1. Introduction

Laser Powder Bed Fusion (PBF-LB/M) is getting uprising attention in industrial applications, as the freedom of design, various processing materials and good mechanical properties are advantageous in comparison to conventional manufacturing technologies (Zhou et al., 2024). Applications range from rapid prototyping, aviation and aerospace to lightweight components with functional integration (Blakey-Milner et al., 2021, Adelmann et al., 2022). For the generation of lightweight components, unit cells, gyroid structures or in general triply periodic structures are used, as part properties like, e.g., stiffness, weight and mechanical properties can be adjusted. As several studies report on static mechanical properties of different unit cells and gyroid structures and fracture behaviour, dynamic mechanical properties often remain unreported (Liu et al., 2017; Mazur et al., 2016; Ma et al., 2019). However, for a comprehensive understanding of mechanical properties and reliable application, the fatigue behaviour is of upmost importance.

For the fatigue behaviour, inlaying porosities and surface quality are decisive factors, as micro-notches, superficial cracks and melting errors lead to crack initiation and propagation until a final failure of the components (Yang et al., 2020). Due to the melting process and adhered powder particles, the surface quality of PBF-LB/M built components is inferior, diminishing the fatigue behaviour. To exclude disadvantages like that, hybrid additive manufacturing technologies are generated, exploiting additive and subtractive manufacturing (Smith et al., 2024). A promising hybrid approach combines PBF-LB/M with an in-situ high-speed milling process, directly machining fabricated components and inlaying surface structures (Wüst et al., 2020; Sommer et al., 2024).

Against this background, we report on a study of mechanical properties of different lattice structures. Different packing densities as well as PBF-LB/M and hybrid built components are compared, evaluating the static and dynamic mechanical load behaviour. For this, compressive strength, different regimes of fatigue and the endurance limit of the structures are determined. Furthermore, differences are discussed based on fractographic and surface analysis.

2. Materials and Methods

Hybrid additive manufacturing is performed using a Lumex Avanace-25 (Matsuura, Fukui, Japan), as schematically depicted in Fig. 1a. The machining unit combines PBF-LB/M with in-situ high-speed milling, generating an alternating additive/subtractive machining process. The PBF-LB/M-process is conducted with a laser power of P_L = 320 W, a scan-speed of v_s = 700 mm/min, a hatch distance of d_h = 140 µm and a layer height of h_l = 50 µm, using an Yb-fibre laser with a nominal spot size of d_{spot} = 200 µm. As a subtractive process is following, a material allowance of a_{total} = 250 µm must be added onto the constructed geometry.

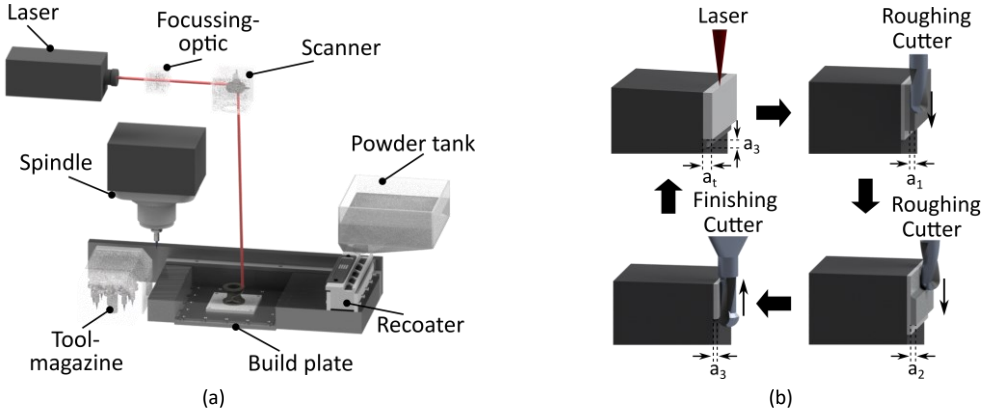

Fig. 1. (a) Hybrid manufacturing unit, integrating a high-speed milling spindle, and (b) in-situ milling process, interrupting the PBF-LB/M-process for the three-step milling process

For the hybrid approach, the PBF-LB/M-process is interrupted after several layers, directly machining the components within the powder bed. Within three milling steps, the material allowance is detached gradually, as two roughing processes remove a_{1+2} = 220 µm, while the finishing step finalises the geometry with an infeed of a_3 = 30 µm (cf. Fig. 1 b). For the three milling processes, a feed rate of v_c = 240 µm, a spindle speed of n = 9,600 1/min and z-pitches of $a_{e,z}$ = 150 µm, 100 µm and 80 µm are employed.

Lattice structures following the Body centered cubic (BCC) unit cell are manufactured, as depicted in Fig. 2a and 2b. Different packing densities are realized, maintaining a nominal relative density of ρ_{rel} = 22 %. For the evaluation of the hybrid approach, the in-situ milling enables a machining of the single struts, not accessible after a finished build process. Please note that, due to the 3-axis system only side and up-facing surfaces are milled (cf. Fig. 2c).

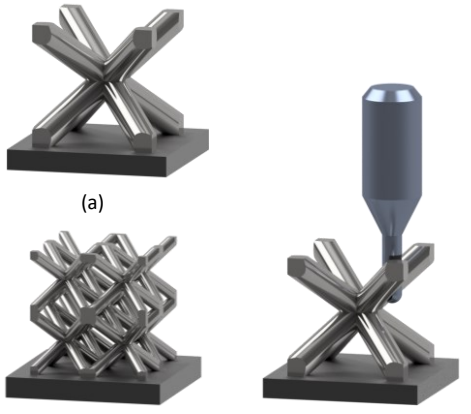

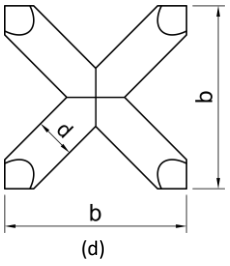

	d / mm	b / mm	A / mm²	ρ_{rel} / %
BCC 1	2.7	12	144	22
BCC 2	1.35	6	144	22

(e)

Fig. 2. a) BCC1 unit cell, b) BCC2 Lattice structure, c) Milling of lattice structures, d) schematic illustration of geometrical parameters, and e) geometrical parameters for the manufactured lattice structures

Static mechanical testing is performed with an AG-X plus universal testing machine (Shimadzu, Kyoto, Japan) with a maximum applied Force of F_{max} = 50 kN for a batch of 5 specimens for each lattice structure. For dynamic testing, an electrodynamic actuator UD020 (Step Engineering, Resana, Italy) is employed, applying a maximum force of F_{max} = 14 kN with a sinusoidal oscillation with a frequency of f = 100 Hz. While the fatigue behaviour is tested, using staircase sequences, the endurance limit is determined by the staircase-method (Caliskan et al., 2021) and a limiting number of cycles of $n = 1.5 \cdot 10^7$.

3. Results and Discussion

The static mechanical load behaviour is shown in Fig. 3a, evaluating the compressive stress-strain response of the lattice structures. At first, the ductile load behaviour of IN718 can be observed for the different structures, as the lattice structures get compressed stepwise up to the maximum applicable stress. Within this, the structure collapses with a deformation of the single struts, not showing an outbreak of component parts.

The BCC1 lattice shows a breakage of the single struts, developing a plateau stress of σ_p = 22.93 MPa and a second small increase for the collapse of the second layer of struts. For the BCC2, the layerwise collapse develops with a more continuous deformation, as smaller layers with a higher number of struts crush. The plateau stress can be determined to σ_p = 61.27 MPa, as a higher packing density increases the static load behaviour significantly. The applied load is distributed across a higher number of knots, decreasing the stress concentration for each and improving the maximum applicable load for an analogous relative density of the lattice structures (Mazur et al., 2016).

For the fatigue behaviour, the trend differs, as depicted in Fig. 3b. Depending on the determination of the Low Cycle Fatigue (LCF) regime up to a number of cycles of $n = 1 \cdot 10^4$, the LCF regime of the BCC2 structures is defined with an amplitude of σ = 37 MPa and merges into the High Cycle Fatigue (HCF) regime. Within this, the Wöhler-line gets described by the gradient of k = −3.53 down to an amplitude of about 9 MPa. As a failure does not occur at lower amplitudes, the endurance limit is evaluated with σ_D = 8.00 MPa, according to the staircase-method. For the BCC1, the LCF regime is identified at a lower amplitude of σ = 30 MPa, accomplishing the HCF regime at about $n = 3.5 \cdot 10^4$. As the Wöhler-line is described by the gradient k = −4.44, the BCC1 shows an improved HCF regime, intersecting the Wöhler-line of the BCC2 structures. Furthermore, the endurance limit can be raised marginally up to σ_D = 8.75 MPa.

As an interims conclusion, while a higher packing density leads to an increased static mechanical load behaviour due to a better distribution of the applied load, the endurance limit is diminished by lower strut diameters, as crack propagation can lead to an early failure of the component. At constant relative density, an increased strut diameter predominates the fatigue behaviour in comparison to the packing density, even though, a decreased compressive strength is evaluated during static testing.

For the static testing of hybrid manufactured components, the deformation behaviour shows, analogous to PBF-LB/M built components, a layer-wise deformation in two stages, as depicted in Fig. 3. For the hybrid manufacturing approach, the plateau stress is determined with σ_p = 40.13 MPa, increasing the compressive strength with about $\Delta\sigma_p$ = 18 MPa. Within the dynamic testing, the LCF regime can be defined with a number of cycles of $n = 5.8 \cdot 10^4$ at the static plateau stress. The HCF regime gets described by a gradient of k = −6.49, improving the deviations of the performed cycle numbers significantly in comparison to the PBF-LB/M built components. Finally, the endurance limit is determined at σ_D = 18.75 MPa, multiplying the endurance limit by the factor of 2.14.

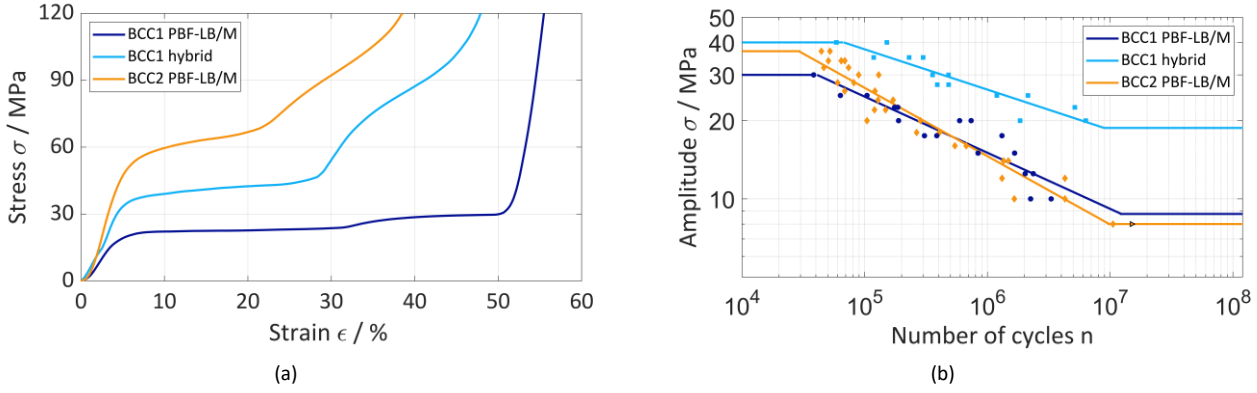

Fig. 3. (a) Stress-Strain diagram, and (b) Wöhler-diagram for the testing of BCC2, BCC1 and hybrid built BCC1 lattice structures

The hybrid additive manufacturing enhances the mechanical properties of the lattice structures, as the improvement of the surface quality leads to higher mechanical resistance (Sarkar et al., 2019). Due to the in-situ high-speed milling, the surface roughness can be minimized from R_a = 17.3 µm for the PBF-LB/M process down to R_a = 0.81 µm for the hybrid manufactured components. As a material allowance of a_t = 250 µm gets detached by the different steps of the milling processes, superficial cracks and micro-notches can be eliminated. Furthermore, melting errors as well as the balling effect of the PBF-LB/M process is prevented, constituting crack initiation and propagation points within mechanical stress.

The geometry of the BCC structures causes a downfacing surface, diminishing the surface roughness, as overhanging structures show an inferior melting quality. The fractographic analysis in Fig. 4a shows that a crack initiation can be observed at the downfacing surface, emanating into the component within the HCF regime (σ = 10 MPa). While the crack propagation weakens the structure, a forced fracture of the up-facing part is identified, developing by virtue of the final failure of the strut. As the 3-axis milling system enables a manufacturing of the up-facing and lateral surfaces, the overhanging structure cannot be improved. Nevertheless, a significantly higher amplitude (σ = 20 MPa) is performed by the hybrid built component, until a crack initiation is developed. As depicted, the crack is, again, emanating from the lower part of the strut, propagating into the material until a final failure occurs.

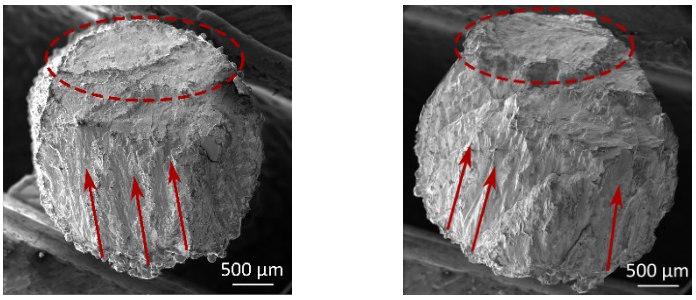

(a) (b)

Fig. 4. SEM-images of crushed struts of (a) PBF-LB/M built, and (b) hybrid built structures, showing a crack initiation and propagation into the strut, leading to a forced fracture at the top of the struts (red zone)

4. Conclusion

In this study, an investigation of mechanical properties of IN718 lattice structures is presented, evaluating the impact of packing density as well as hybrid manufacturing on the static and dynamic load behaviour. For this, BCC lattice structures are manufactured with different packing densities and continuous relative density, comparing the compressive strength and the sole PBF-LB/M and hybrid built components.

While a higher packing density leads to an increased maximum compressive strength, a greater strut diameter leads to an improved fatigue behaviour. Additionally, the in-situ high-speed milling is leading to enhanced mechanical properties, as the compressive strength as well as the fatigue behaviour are considerably increased. Due to the superior surface quality of the hybrid built components, the plateau stress is improved by 75 % up to a maximum of 40.1 MPa and the endurance limit is increased by the factor 2.14 to 18.75 MPa. As superficial cracks and melting errors are excluded by the hybrid approach, the mechanical properties are improved significantly. Crack initiation and propagation can be reduced, as shown in the fractographic analysis.

References

Adelmann, B.; Hellmann, R. 2022. Function Integration in Additive Manufacturing: Design and Realization of an LPBF Built Compressed Air Motor, Materials, 15 (19), doi: 10.3390/ma15196632.

Blakey-Milner, B.; Gradl, P.; Snedden, G.; Brooks, M.; Pitot, J.; Lopez, E.; Leary, M.; Berto, F.; Du Plessis, A. 2021. Metal additive manufacturing in aerospace: A review, Materials & Design, 209, S. 110008. doi: 10.1016/j.matdes.2021.110008.

Caliskan, S.; Gürbüz, R. 2021. Determining the endurance limit of AISI 4340 steels in terms of different statistical approaches, Fracture and Structural Integrity, 15(58), 344–364. doi: 10.3221/IGF-ESIS.58.25

Liu, L.; Kamm, P.; García-Moreno, F.; Banhart, J.; Pasini, D. 2017. Elastic and failure response of imperfect three-dimensional metallic lattices: the role of geometric defects induced by Selective Laser Melting, Journal of the Mechanics and Physics of Solids, 107, S. 160–184. doi: 10.1016/j.jmps.2017.07.003.

Ma, S.; Tang, Q.; Feng, Q.; Song, J.; Han, X.; Guo, F. 2019. Mechanical behaviours and mass transport properties of bone-mimicking scaffolds consisted of gyroid structures manufactured using selective laser melting, Journal of the Mechanical Behavior of Biomedical Materials, 93, S. 158–169. doi: 10.1016/j.jmbbm.2019.01.023.

Mazur, M.; Leary, M.; Sun, S.; Vcelka, M.; Shidid, D.; Brandt, M. 2016. Deformation and failure behaviour of Ti-6Al-4V lattice structures manufactured by selective laser melting (SLM), The International Journal of Advanced Manufacturing Technology, 84 (5), S. 1391–1411. doi: 10.1007/s00170-015-7655-4.

Sarkar, S.; Kumar, C.S.; Nath, A.K. 2019. Effects of different surface modifications on the fatigue life of selective laser melted 15–5 PH stainless steel, Materials Science and Engineering: A, 762, S. 138109. doi: 10.1016/j.msea.2019.138109.

Smith, S.; Schmitz, T.; Feldhausen, T.; Sealy, M. 2024. Hybrid metal additive/subtractive machine tools and applications, CIRP Annals, 73 (2), S. 615–638. doi: 10.1016/j.cirp.2024.05.002.

Sommer, D.; Hornung, S.; Esen, C.; Hellmann, R. 2024. Surface roughness optimization of hybrid PBF-LB/M-built Inconel 718 using in situ high-speed milling, Int J Adv Manuf Technol, 132 (3-4), S. 1741–1751. doi: 10.1007/s00170-024-13382-5.

Wüst, P.; Edelmann, A.; Hellmann, R. 2020. Areal Surface Roughness Optimization of Maraging Steel Parts Produced by Hybrid Additive Manufacturing, Materials, 13 (2), S. 418. doi: 10.3390/ma13020418.

Yang, K.; Huang, Q.; Wang, Q.; Chen, Q. 2020. Competing crack initiation behaviors of a laser additively manufactured nickel-based superalloy in high and very high cycle fatigue regimes, International Journal of Fatigue, 136, S. 105580. doi: 10.1016/j.ijfatigue.2020.105580.

Zhou, L.; Miller, J.; Vezza, J.; Mayster, M.; Raffay, M.; Justice, Q. et al. 2024. Additive Manufacturing: A Comprehensive Review, Sensors (Basel, Switzerland), 24 (9). doi: 10.3390/s24092668.